Cell, Vol. 88, 675–684, March 7, 1997, Copyright ©1997 by Cell Press

Cell Cycle–Dependent Polar Localization of Chromosome Partitioning Proteins in Caulobacter crescentus

Dane A. Mohl and James W. Gober
Department of Chemistry and Biochemistry
and Molecular Biology Institute
University of California
Los Angeles, California 90095-1569

Summary

In the bacterium C. crescentus, the cellular homologs of plasmid partitioning proteins, ParA and ParB, localize to both poles of the predivisional cell following the completion of DNA replication. ParB binds to DNA sequences adjacent to the origin of replication suggesting that this region of the genome is tethered to the poles of the cell at a specific time in the cell cycle. Increasing the cellular levels of ParA and ParB disrupts polar localization and results in defects in both cell division and chromosome partitioning. These results suggest that ParA and ParB are involved in partitioning newly replicated chromosomes to the poles of the predivisional cell and may function as components of a bacterial mitotic apparatus.

Introduction

Following DNA replication in bacterial cells, the new sister chromosomes physically separate and then efficiently partition to each pole of the predivisional cell (reviewed in Hiraga, 1992; Rothfield, 1994; Wake and Errington, 1995). This process must be precisely coordinated with cell division to ensure that each daughter cell receives its own copy of the chromosome. Separation of the chromosomes involves the removal of DNA catenanes at the replication termini and requires both the activity of topoisomerases and replication terminus-specific recombination events. The mechanisms that subsequently result in partitioning of the newly separated chromosomes are not as well understood. Unlike eukaryotic cells, a well-defined spindle or other structure involved in directing the nascent chromosomes to the poles of the cell has not been identified. Movement of the chromosomes to the poles of the predivisional cell has been attributed to both the relatively nonspecific attachment of nucleoids to the growing cell envelope (Woldringh and Nanninga, 1985; Begg and Donachie, 1991) or to a motor-like protein, such as MukB (Hiraga et al., 1989; Niki et al., 1991, 1992). When the gene encoding MukB is deleted in E. coli, the result is a significant number of anucleate cells in culture (Niki et al., 1991). The amino-terminal portion of MukB contains a consensus nucleotide binding motif and possesses significant sequence homology to dynamin, a microtubule-associated protein isolated from rat brain (Niki et al., 1992). These observations have led to the hypothesis that MukB functions as at least one of the locomotor proteins that pushes or pulls the newly replicated chromosomes toward the cell poles. MukB has been shown to bind nonspecifically to DNA in vitro (Niki et al., 1992). It is unlikely that this nonspecific DNA binding contributes significantly to partitioning the chromosome. This conclusion is based on the observation that plasmids containing the E. coli origin of replication (*oriC*) fail to partition efficiently, suggesting that a specific centromere-like sequence is required for partitioning.

In addition, some bacteria possess homologs of two plasmid partitioning genes, *parA* and *parB*. In single or low copy-number plasmids such as F factor, R1, RK2, or the prophage form of bacteriophage P1, these gene products (*parA* and *parB* in P1) are required for the efficient partitioning of newly replicated episomes to each daughter cell (Austin and Abeles, 1983a, 1983b; Gerdes and Molin, 1986; Mori et al., 1989; Schmidhauser et al., 1989). Experiments using purified ParA have demonstrated that it possesses a weak ATPase activity in vitro (Davis et al., 1992; Watanabe et al., 1992). ATPase activity can be stimulated in the presence of purified *parB* gene product, indicating that these two proteins probably interact with each other in vivo (Davis et al., 1992). *parB* encodes a sequence-specific DNA binding protein (Martin et al., 1987; Davis and Austin, 1988). For example, the *parB* gene product from the prophage form of E. coli bacteriophage P1 binds to repeated sequences of dyad symmetry (*parS*) located downstream of the *parB* coding region (Martin et al., 1987; Davis and Austin, 1988). Sequences of this type have been identified adjacent to the *parAB* operon of several different plasmids. Mutant plasmids with deletions in this *cis*-acting region cannot be stably maintained. Additionally, mini R1 and P1 plasmids containing only the *parS* sequence (or *parC* in the case of R1) do not partition efficiently unless the *parA* and *parB* gene products are supplied in *trans* (Martin et al., 1987; Dam and Gerdes, 1994). Therefore, these experiments suggest that the *parS* sequence functions as a centromere during plasmid partitioning.

From these experiments a general view of the mechanism of plasmid DNA partitioning has emerged. First, the *parB* gene product is envisioned as binding to the *parS* centromere sequence during partitioning. The ParB-DNA complex then presumably interacts with a cellular receptor that is, in turn, directed away from the mid-cell region toward the cell poles. The identity of this receptor and the mechanism of locomotion that directs plasmid DNA toward opposite cell poles is not known. The role of the *parA* gene product in partitioning is also unknown, however it may be involved in forming a complex with ParB, the centromere, and the putative receptor. Another possible model is that ParA itself functions as the receptor for the ParB-DNA complex.

Homologs of these two genes have been previously identified in a sequence analysis of DNA adjacent to the origin of replication in Pseudomonas putida (Ogasawara and Yoshokawa, 1992) and as genes important for spore development in Bacillus subtilis (*soj* and *spo0J*) (Mysliwiec et al., 1991). The genetic organization of these *parAB* homologs appears to be similar to that of plasmids, including the presence of inverted repeat sequences downstream of the *parB* coding sequence that could serve as a ParB binding site. Interestingly, the *parAB* homologs in B. subtilis were previously identified

genetically as regulators of an early step in sporulation (Mysliwiec et al., 1991; Ireton et al., 1994). In the absence of Spo0J, Soj prevents the activation of the sporulation transcription factor Spo0A (Ireton et al., 1994). The activation of Spo0A is regulated by both nutritional cues as well as the initiation of DNA replication. This raises the intriguing possibility that these gene products may function in a developmental checkpoint that links chromosome partitioning to the initiation of sporulation. In B. subtilis, experimental evidence has demonstrated that *soj* and *spo0J* play a role in the partitioning of chromosomes during both vegetative growth and sporulation (Ireton et al., 1994; Sharpe and Errington, 1996). For example, mutants deficient in *spo0J* show a mild chromosome partitioning defect, generating about 3% anucleate cells during vegetative growth (Ireton et al., 1994).

In order to determine the role of *parA* and *parB* in the process of chromosomal partitioning, we have cloned their cellular homologs from the developmental bacterium Caulobacter crescentus. C. crescentus is an ideal bacterial model system to examine chromosomal DNA partitioning since cell cycle–synchronized populations are easy to obtain and manipulate experimentally. We show that purified ParB binds specifically to DNA sequences downstream of the *parAB* operon, which is located within 80 kbp of the origin of replication. Cell cycle immunolocalization experiments show that the subcellular distribution of ParB changes during the cell cycle exhibiting a periodic bipolar localization pattern in late predivisional cells following the completion of DNA replication. ParA is also found concentrated at both poles of the predivisional cell. To examine whether the correct temporal and spatial distribution of ParA and ParB was required for chromosome partitioning, we induced the mislocalization of these proteins by increasing their cellular concentrations. Under these conditions, the cells exhibited a relatively severe DNA partitioning defect. Therefore, ParA and ParB may function as components of a mitotic-like apparatus in bacterial cells.

Results and Discussion

In C. crescentus, *parA* and *parB* map to a region that is within 80 kbp of the origin of replication and, as in plasmids and other organisms, are organized in an operon (Figure 1). Immediately downstream of the coding sequence is a relatively A+T-rich stretch of DNA (49% A+T within 200 bp) that could serve as a ParB binding site. Aside from the A+T content, this region does not exhibit similarity to the well-defined ParB binding sites present in low copy number plasmids. The predicted amino acid sequence of *parA* is 50% identical to *soj* of B. subtilis and 15% to 21% identical to the *parA* homologs of plasmids (Figure 2A). *parB* is predicted to share 45% identity with *spo0J* and 20% to 25% identity with its plasmid homologs (Figure 2B). Unlike *soj* and *spo0J* in B. subtilis, both *parA* and *parB* are essential genes in C. crescentus. To test whether *parA* or *parB* is essential, we attempted to create null mutations by integrating an internal DNA fragment of each gene by homologous recombination. Internal fragments (400 bp) of the coding region of each gene were isolated using PCR. These

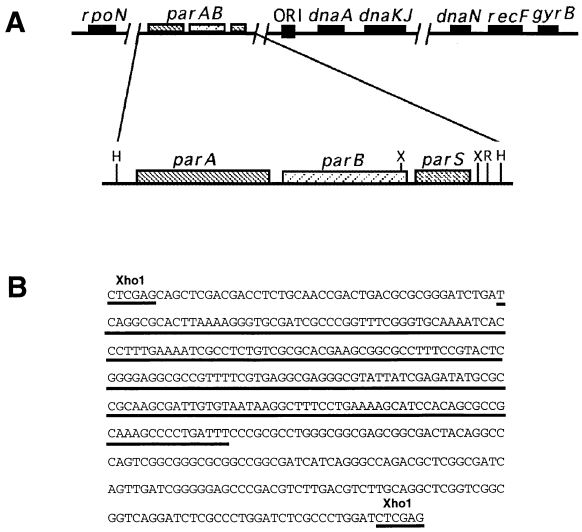

Figure 1. Organization of the *parAB* Operon and Sequence of the *parS* Region

(A) Genetic organization of the C. crescentus *parAB* operon. The chromosomal location of *parAB* was mapped by hybridization of *parAB* coding DNA to a pulse field gel of digested chromosomal DNA. As in Pseudomonas putida (Ogasawara and Yoshokawa, 1992) and Bacillus subtilis (Mysliwiec et al., 1991), the C. crescentus homologs of *parAB* lie adjacent to the origin of replication (ORI). Immediately downstream of the *parAB* coding region is a noncoding DNA sequence, *parS*, which functions as a ParB binding site. H, HindIII; R, EcoR1; X, XhoI.

(B) DNA sequence of the *parS* region. Underlined is the relatively A+T-rich region (49% A+T) that may serve as a ParB binding site.

were subcloned into the suicide plasmid pJM21 (Alley et al., 1993) and introduced in C. crescentus by conjugation. Transconjugants that were kanamycin resistant contained an integrated plasmid that disrupted the coding sequence of either *parA* or *parB*. We were unable to obtain null mutations within the *parAB* operon by this method unless another wild-type copy of either *parA* or *parB* was present on a plasmid containing the HindIII-EcoRI fragment (Figure 1A) or at another location on the genome, indicating that these two genes are required for cell viability. In order to ensure that integrations in the *parA* coding sequence were not polar on *parB*, we also constructed a strain that contained the *parB* coding sequence in *trans* on a plasmid or at another location in the genome (*xyl* operon). In both cases we were unable to obtain disruptions in the *parA*, indicating that *parA* is an essential gene and that integrations at the parA locus do not have downstream polar effects.

ParB Binds to DNA Sequences near the Origin of Replication

In plasmids, the binding of ParB to *parS* DNA sequences 3′ to the *parAB* operon is essential for efficient partitioning. We wished to test whether C. crescentus ParB functions in a similar fashion. To accomplish this, we performed a gel mobility shift experiment using purified ParB and a 420 bp labeled XhoI fragment (Figure 1) that contained the A+T-rich DNA sequences immediately downstream of the parB coding region. ParB formed a concentration-dependent, specific gel shift complex with DNA downstream of the *parAB* operon that could

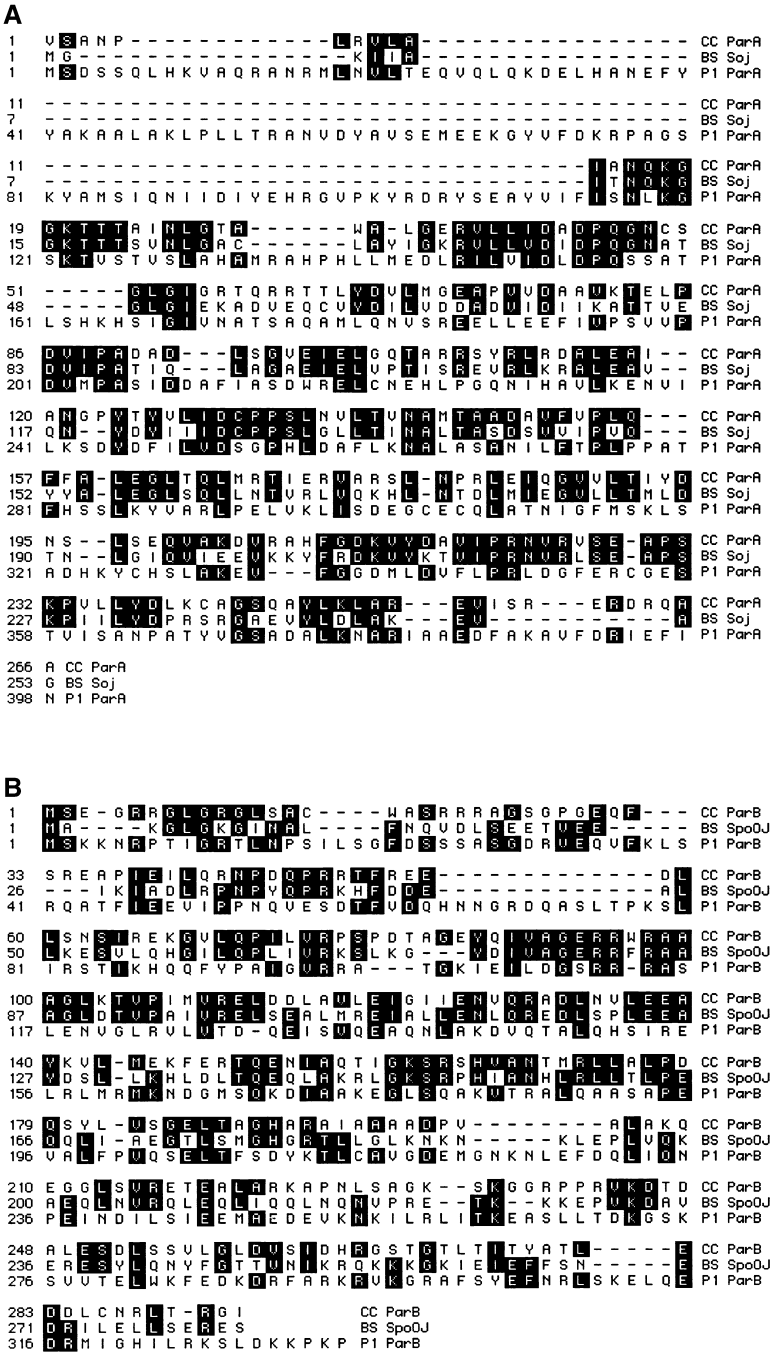

Figure 2. Sequence Alignment of ParA and ParB

(A) The predicted amino acid sequence of ParA from C. crescentus (CC) is shown aligned with Soj from B. subtilis (BS) and ParA from bacteriophage P1 (P1).

(B) The predicted amino acid sequence of C. crescentus ParB (CC) is shown aligned with Spo0J from B. subtilis (BS) and ParB from bacteriophage P1 (P1). Alignments were performed by the CLUSTAL method (Higgins and Sharp, 1988).

not be competed away with nonspecific DNA (Figure 3A). Since these sequences are relatively A+T-rich, we tested whether ParB could bind to other A+T-rich sequences by performing a gel mobility shift assay using a 280 bp DNA fragment that contained the *fliF* operon promoter. This region possesses an A+T content that is comparable to the *parS* region. In this assay, we detected weak binding of purified ParB to the *fliF* promoter fragment (Figure 3B). At the highest concentration of ParB used, approximately six times less labeled *fliF* DNA was bound compared to *parS* DNA. In another experiment, we tested whether *fliF* DNA could compete with ParB binding to the *parS* fragment (Figure 3C). In this case, labeled *fliF* and *parS* DNA were incubated together with purified ParB. We assayed binding by quantitating the amount of unbound probe remaining following incubation with ParB. ParB bound preferentially to the labeled *parS* DNA fragment. Approximately 90% of the *parS* DNA was bound by ParB compared to 5% of the labeled *fliF* DNA fragment. These experiments indicate that ParB binds to the *parS* region downstream of the *parAB* operon. Furthermore, ParB is capable of binding weakly to a DNA fragment that contains A+T-rich sequences, raising the possibility that, in addition to *parS*, there may exist other possible ParB binding sites within the C. crescentus genome.

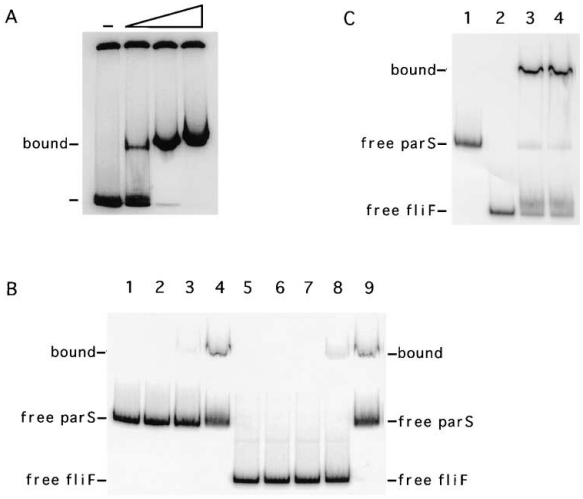

Figure 3. ParB Binds to DNA Sequences 3′ to the ParAB Operon

(A) Gel mobility shift analysis was performed to determine whether ParB binds to DNA sequences downstream of the *parAB* operon. Various concentrations of purified his-tagged ParB were incubated with a 420 bp, end-labeled, XhoI *parS* DNA fragment (Figure 1B) in the presence of both single stranded (1.8 μg/μl) and double-stranded competitor DNA (0.3 μg/μl) (see Experimental Procedures), the reaction mixture was subjected to electrophoresis, and the dried gel exposed to X-ray film. Free (unbound) and bound probe are indicated. Left lane (−): no protein added. Next three lanes: 0.03, 0.09, and 0.17 nmol his-ParB added, respectively.

(B) Assay of ParB binding to A+T-rich DNA. Various concentrations of purified his-tagged ParB were incubated with either a 420 bp end-labeled, XhoI *parS* DNA fragment (2.5 nM) (lanes 2–4; 0.03, 0.09, and 0.17 nmol his-ParB added, respectively) or a 280 bp HindIII-BamHI *fliF* operon promoter fragment (2.5 nM) (lanes 6–8; 0.03, 0.09, and 0.17 nmol his-ParB added, respectively). Lanes 1 and 5 contained, repectively, *parS* or *fliF* DNA incubated without ParB. Incubations and gel mobility shift were performed as described in Experimental Procedures except that 3 μg/μl of sheared salmon sperm DNA was used as a nonspecific competitor. Lane 9: *parS* DNA incubated in the presence of 0.17 nmol ParB, with salmon sperm DNA, single-stranded DNA, and pUC19 DNA (0.4 μg) as competitors.

(C) *parS* and *fliF* competition assay. Gel mobility shift analysis was performed after incubating the labeled *parS* and *fliF* DNA fragments together with purified ParB. Lane 1, *parS* DNA, no protein added; lane 2, *fliF* DNA, no protein added; lanes 3–4, *parS* and *fliF* DNA incubated with 0.17 nmol his-ParB. Following phosphorimager analysis, the amount of DNA bound was calculated by subtracting the amount of unbound probe remaining. In both lanes, ParB, bound approximately 90% of the *parS* DNA fragment and 5% of the *fliF* DNA fragment.

Biochemical experiments using the plasmid homologs of ParA and ParB have shown that these two proteins interact with each other (Davis et al., 1992). One possibility is that ParA and ParB form a complex at the *parS* sequence that functions in partitioning. To test this idea we examined whether purified ParA could supershift the ParB-*parS* complex. We were however unable to detect a ParA-ParB-*parS* complex using this assay. Furthermore, the addition of ATP or ADP did not stimulate the formation of a ParA-ParB complex. These results indicate that ParB may, by itself, function by binding to a region of the genome adjacent to the origin of replication. Alternatively, ParA and ParB may form a complex in vivo only when in association with another cellular component.

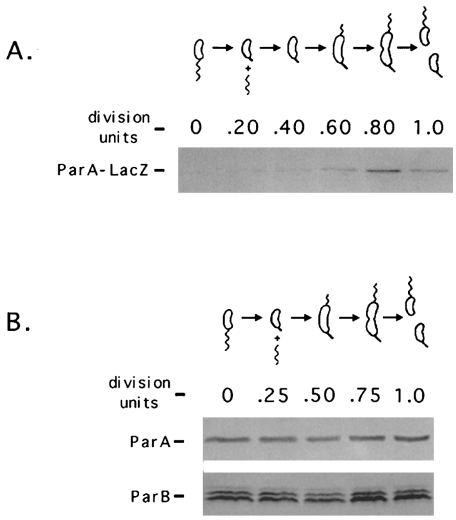

Figure 4. Cell Cycle Expression of *parA* and *parB*

(A) Expression of the *parAB* operon is under cell cycle control. Cells containing a parA-lacZ fusion were synchronized and permitted to progress through the cell cycle. At 0, 30, 60, 90, 120, and 150 min, a portion of the culture was removed and proteins were pulse-labeled with ^{35}S-*trans* label. Labeled β-galactosidase was immunoprecipitated and subjected to electrophoresis. Indicated are the cell types present at each time point as assayed by light microscopy.

(B) The levels of ParA and ParB do not change during the course of the cell cycle. The levels of ParA and ParB in synchronized cultures were assayed by immunoblot using antibodies directed against ParA or ParB. Indicated are the cell types present at each time point as assayed by light microscopy.

Cell Cycle Expression of *parA* and *parB*

Since ParA and ParB may be required at a specific stage of the cell division cycle, we examined their expression pattern during the cell cycle using synchronized populations of cells. C. crescentus undergoes a characteristic asymmetric cell division resulting in the formation of two dissimilar progeny cells, a motile flagellum-bearing swarmer cell and a nonmotile stalked cell (reviewed in Gober and Marques, 1995). In progeny swarmer cells, the reinitiation of chromosomal DNA replication is silenced for a defined period of time. Following this interval (~45 min at 30°C), the flagellum is shed, a stalk is synthesized in its place, and DNA replication is initiated. Cell division then follows within 90 min, generating the two distinct progeny cells. We synchronized C. crescentus by isolating pure populations of swarmer progeny cells and permitting them to progress through the cell cycle. To test whether transcription of the *parAB* operon was expressed under cell cycle control, a *parA-lacZ* fusion was introduced. The cells were synchronized; at various times thereafter an aliquot was removed and pulse-labeled with ^{35}S-*trans* label, and labeled β-galactosidase was immunoprecipitated. The expression of this fusion was under cell cycle control, with relatively low levels of expression in swarmer cells and newly formed stalked cells. Expression peaked in late predivisional cells and then declined after cell division (Figure 4A). Using immunoblot on cell extracts obtained from synchronized populations, we then determined the levels of ParA and ParB during the cell cycle. Interestingly, although transcription was under cell cycle

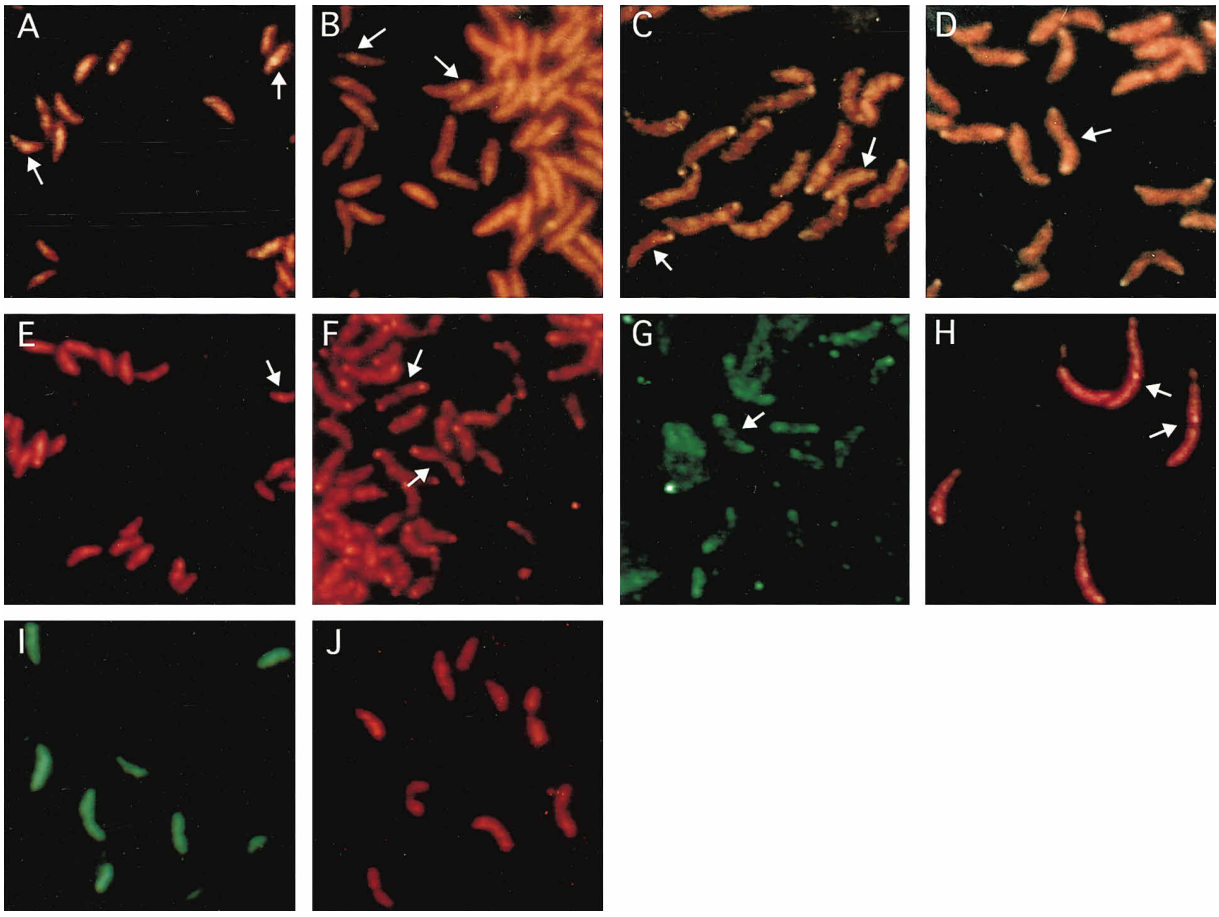

Figure 5. Localization of ParA and ParB by Fluorescence Microscopy

The first four panels (A–D) show immunolocalization of ParB during the course of the cell division cycle. ParB was stained with fluorescein-conjugated secondary antibody. The cells were stained with propidium iodide. (A) Immunolocalization of ParB in swarmer cells (0 min following synchronization, see text). Most cells exhibit a diffuse staining pattern. The arrows indicate staining of some cells at the midcell. (B) Immunolocalization of ParB in stalked cells (60 min following synchronization). The arrows indicate staining at the midcell or one pole. (C) Immunolocalization of ParB in predivisional cells (90 min following synchronization). The arrows indicate cells with staining at a single pole. (D) Immunolocalization of ParB in late predivisional cells (120 min following synchronization). The arrow indicates a cell with staining at both poles. (E) Immunolocalization of ParB in synchronized swarmer cells showing staining of streptavidin–Texas red bound to biotinylated secondary antibody. The arrow indicates a cell with staining at the midcell. (F) Immunolocalization of ParB in late predivisional cells showing staining of streptavidin–Texas red bound to biotinylated secondary antibody. The cells depicted are the same experiment as those in (E) harvested 120 min later. The arrows indicate cells with staining at both poles. (G) Immunolocalization of epitope-tagged ParA in a mixed population of cells showing staining of fluorescein-conjugated secondary antibody. The arrow indicates a cell with a bipolar staining pattern. (H) Immunolocalization of ParB in cells treated with the DNA replication inhibitor hydroxyurea showing staining of streptavidin–Texas red bound to biotinylated secondary antibody. A mixed population of cells was treated with 10 μg/ml hydroxyurea (final concentration) for 6 hr. The arrows indicate elongated cells with staining at the midcell. (I) Immunofluorescence microscopy of cells expressing a *gyrB-lacZ* fusion showing diffuse staining of fluorescein-conjugated secondary antibody. (J) Immunofluorescence microscopy of cells expressing a *gyrB-lacZ* fusion showing diffuse staining of streptavidin–Texas red bound to biotinylated secondary antibody.

control, the levels of both ParA and ParB did not change appreciably during the course of the cell cycle (Figure 4B), suggesting that a critical cellular concentration of both proteins must be maintained (see section below). Interestingly, the ParB immunoblot exhibited several species with differing mobilities indicating that it may be subject to covalent modification. The relative abundance of these forms, however, did change during the cell cycle (Figure 4B).

Subcellular Distribution of ParA and ParB during the Cell Cycle

DNA partitioning in bacteria involves the movement of newly replicated chromosomes toward the cell poles. ParA and/or ParB may therefore exist at distinct cellular locations during different periods of the cell cycle. In one simple model, we envision that movement of ParA and ParB parallels that of the newly replicated chromosomes. To test for subcellular localization of ParB during the cell cycle, we performed immunofluorescence microscopy on synchronized cell populations with anti-ParB antibody (Figure 5). ParB antibody complexes were visualized using a secondary antibody conjugated to fluorescein isothiocyanate (Figures 5A–5D). In swarmer cells ($t = 0$ min) where DNA replication does not occur, ParB was for the most part distributed throughout the cell, although a minority of cells showed some localization at the midcell or at a pole (Figures 5A and 2E). At

Table 1. Subcellular Distribution of ParB during the Cell Division Cycle

	Time (min)	Stage	Localization Pattern (%)		
			Midcell	Single pole	Bipolar
Fluorescein	0	swarmer	20	9	0
	60	stalked	7	10	0
	90	early prediv.	0	36	20
	120	late prediv.	0	16	43
Texas red	0	swarmer	6	3	0
	120	late prediv.	0	26	51

this time point, 20% of the cells exhibited localization of ParB at the midcell and 9% at a single pole (Table 1). Localization was not observed in the remaining 71% of the population. In stalked cells, following the initiation of DNA replication (t = 60 min), a similar pattern of ParB localization was observed (Figure 5B). The majority of cells exhibited no localization (83%) and, in a minor fraction, ParB was concentrated at the midcell (7%) or the pole (10%) (Table 1). As DNA replication proceeds, ParB begins to concentrate at one pole of the predivisional cell (Figure 5C); chromosomal DNA replication is approximately half completed in the cells depicted in this panel (t = 90 min). The majority of the cells that contained localized ParB exhibited localization at one pole (36%) (Table 1), whereas 15% exhibited localization at both poles. Finally, in late predivisional cells (120 min), following the completion of DNA replication, the majority of cells that exhibited localization had ParB distributed to both poles of the predivisional cell (43%) (Figures 5D and 5F). In contrast to early predivisional cells (Figure 5C), only 16% of these late predivisional cells contained ParB concentrated at a single pole. We also performed a similar experiment using biotinylated secondary antibody in conjunction with streptavidin–Texas red in order to visualize ParB (Figures 5E and 5F). Identical results were obtained using this fluorochrome; in swarmer cells (t = 0), very few cells exhibited ParB localization (6% midcell, 3% single pole) (Figure 2E), whereas in late predivisional cells, ParB appeared to be concentrated to both poles in a significant fraction of cells (51% bipolar, 26% single pole) (Figure 5F). Immunofluorescence micrscopy performed on control cells containing a cytoplasmic *gyrB-lacZ* fusion did not exhibit localization (Figures 5I and 5J).

In summary, these experiments demonstrate that the subcellular distribution of ParB changes periodically during the cell division cycle (Table 1). In swarmer cells, which do not replicate DNA, or in stalked cells shortly following the onset of DNA replication, ParB is for the most part not localized within the cell. Then, in early predivisional cells most of the localized ParB is distributed to a single pole of the cell. At this time point a substantial fraction of the chromosome has replicated. Based on previous measurements of the rate of replication (Dingwall and Shapiro, 1989), we estimate that approximately 60% of the genome is replicated by this time in the cell cycle. After replication is essentially complete in late predivisional cells, ParB is localized at both poles of the cell. Therefore the spatial distribution of ParB is coupled to cell cycle events and approximates the movement of the newly replicated chromosomes.

Although we were unable to detect the interaction of ParA and ParB using a DNA binding assay, experiments with purified ParA from bacteriophage P1 have demonstrated that it possesses a weak ATPase activity that can be stimulated in the presence of purified ParB, indicating that these two proteins probably interact with each other in vivo (Davis et al., 1992). If this is also true of the C. crescentus homologs, we expect that ParA would also be localized in a cell cycle–dependent fashion. To test this idea, the subcellular distribution of the epitope-tagged ParA (ParA-M2) was assayed by immunofluorescence microscopy on an unsynchronized population of cells (Figure 5G). ParA-M2 was concentrated at both poles of larger predivisional cells, whereas smaller swarmer cells exhibited a diffuse staining pattern. This suggests that the subcellular distribution of ParA, like ParB, varies during the course of the cell cycle.

Chromosome movement following DNA replication could serve to deliver ParA and ParB bound to DNA toward the poles of the cell. Thus, the polar localization of ParA and ParB should be dependent on DNA replication. To test whether DNA replication was required for ParB localization, we determined the subcellular distribution of ParB in an unsynchronized population of cells that had been treated with the DNA replication inhibitor hydroxyurea (Figure 5H). Hydroxyurea treatment resulted in the formation of elongated cells, with a high proportion containing a single concentrated region of ParB localization at the midcell rather than the usual polar or bipolar pattern. This suggests that polar localization of ParB during the cell cycle is dependent on DNA replication and subsequent movement of the chromosomes. ParA and ParB may be active participants in this process or simply passively localized by chromosome movement.

Increased Expression of ParA and ParB Result in Both Cell Division and Chromosome Partitioning Defects

To test whether ParA and ParB localization was required for chromosome partitioning, we increased the cellular levels of ParA and ParB by controlling their expression with a xylose-inducible promoter (Meisenzahl et al., 1997). We reasoned that this would effectively increase the amount of ParA or ParB in the cell that is not localized to the poles. To test whether this occurred, we determined the localization of ParB in cells that overexpressed either ParA, ParB, or both ParA and -B (Figures 6E, 6H, and 6K). We then examined whether loss of localization of these proteins affected chromosome partitioning and cell division. Cells in which ParA expression

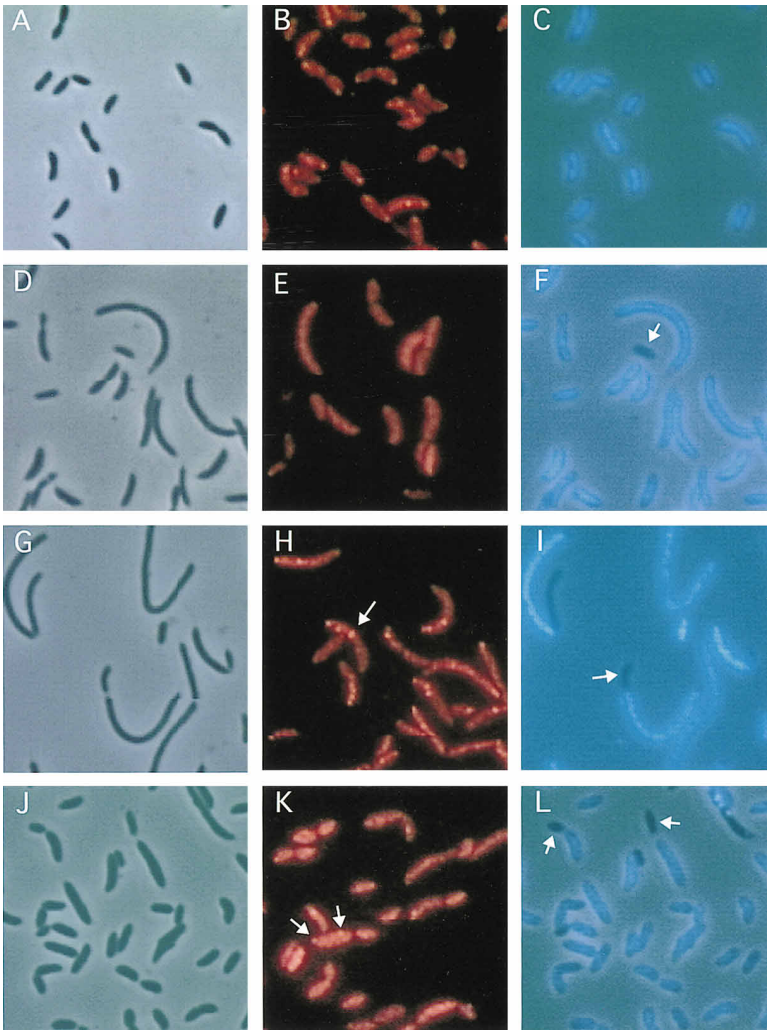

Figure 6. Effect of Increased Levels of ParA and ParB on Cell Growth, ParB Localization and DNA Content

In order to control the expression of *parA* and *parB*, each gene was placed downstream of the *C. crescentus xylA* promoter (Meisenzahl et al., 1997). ParA and ParB expression was induced for 6 hr by the addition of xylose to a final concentration of 1.6 mM in PYE medium. (A–C) Wild-type cells. (A) Phase contrast micrograph of a mid–log phase culture of wild-type cells. (B) Immunolocalization of ParB in a mid-log phase culture of wild-type cells showing staining of streptavidin–Texas red bound to biotinylated secondary antibody. (C) Fluorescence micrograph of the same field as (A) showing DAPI staining as an assay of DNA content. Wild-type cultures typically contain less than 0.05% anucleate cells. (D–F) Cells expressing increased amounts of ParA. (D) Phase contrast micrograph of a mid-log phase culture of cells expressing high levels of ParA. (E) Immunolocalization of ParB in a mid–log phase culture of cells expressing high levels of ParA showing staining of streptavidin–Texas red bound to biotinylated secondary antibody. (F) Fluorescence micrograph of the same field as (D) showing DAPI staining as an assay of DNA content. The arrow indicates an anucleate cell. The frequency of anucleate cells in this population was 5%. (G–I) Cells expressing increased amounts of ParB. (G) Phase contrast micrograph of a mid-log phase culture of cells expressing high levels of ParB. (H) Immunolocalization of ParB in a mid-log phase culture of cells expressing high levels of ParB showing staining of streptavidin–Texas red bound to biotinylated secondary antibody. The arrow indicates a cell exhibiting ParB localization at multiple locations. (I) Fluorescence micrograph of the same field as (G) showing DAPI staining as an assay of DNA content. The frequency of anucleate cells in this population was 5%. (J–L) Cells expressing increased amounts of both ParA and ParB. (J) Phase contrast micrograph of a mid–log phase culture of cells expressing high levels of ParA and ParB. (K) Immunolocalization of ParB in a mid-log phase culture of cells expressing high levels of ParA and ParB showing staining of streptavidin–Texas red bound to biotinylated secondary antibody. The arrows indicate a cell with two concentrated regions of ParB within a single compartment of a predivisional cell. (L) Fluorescence micrograph of the same field as (J) showing DAPI staining as an assay of DNA content. The frequency of anucleate cells in this population was 10%.

was increased exhibited a cell division defect as seen by the appearance of elongated cells in culture following the addition of xylose (Figure 6D) and exhibited mislocalization of ParB (Figure 6E). Most of these cells had ParB distributed throughout the cytoplasm with very few cells exhibiting discrete regions of localization. Increased expression of ParB resulted in a severe cell division defect in which many of the cells were filamentous (Figure 6G). As with the ParA overexpressing strain, these cells exhibited mislocalization of ParB (Figure 6H). Many of these cells had ParB localized to one pole as well as localization to a variable number (ranging from 2 to 8) of regions scattered throughout the cell. These experiments suggest that the cellular levels and possibly the proper spatial location of ParA and ParB may play a crucial role in regulating cell division. To examine whether the loss of polarly localized ParB affects the partitioning of chromosomal DNA, we stained nucleoids with the fluorescent dye DAPI (20). In strains that expressed increased levels of ParA or ParB, there was a defect in chromosome partitioning; each culture produced approximately 5% anucleate cells (Figures 6F and 6I) versus less than 0.05% in wild-type cultures (Figure 6C).

We next examined the effect of increasing the cellular levels of both ParA and ParB. In contrast to strains that overexpressed ParA or ParB alone, the increased expression of both proteins had only a mild effect on cell division (Figure 6J); however, ParB was still mislocalized (Figure 6K). In addition to having ParB distributed randomly throughout the cell, a small fraction of predivisional cells contained ParB concentrated at the pole and the midcell within the same compartment (Figure 6K). These cells, although relatively normal in appearance, exhibited a severe defect in the proper partitioning of chromosomal DNA, generally containing approxi-

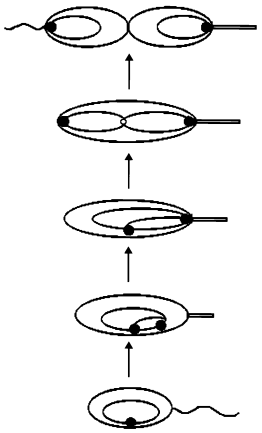

Figure 7. Model Summarizing the Relation between ParA and ParB Localization, Chromosome Movement, and Cell Division

The chromosomes are represented by the ellipses within the cells. ParA and ParB bound to chromosomal DNA are represented by the closed circles. We hypothesize that ParA and ParB form a complex within the cell. This is based on experiments with the plasmid homologs of ParA and ParB which demonstrated that ParB stimulated the ATPase activity of ParA in vitro, suggesting that they interact with each other (Davis et al., 1992). In swarmer cells, before the onset of DNA replication, ParA and ParB are distributed throughout the cell, with very few cells showing localization at the midcell. Following the initiation of DNA replication in stalked cells, the ParAB complex is localized at the midcell region. As replication progresses in predivisional cells, ParAB localizes first to one pole and later in the cell cycle to both poles. ParAB localization may serve to tether one region of the genome, adjacent to the origin of replication, to the poles of the predivisional cell. Thus, the distribution of ParAB during the cell cycle parallels the movement of chromsomal DNA.

mately 10% anucleate cells in culture following the addition of xylose (Figure 6L). Thus it appears that the correct cellular concentration of ParA and ParB is essential for normal cell division and chromosome partitioning. We hypothesize that mislocalization of these proteins as a consequence of increased levels of expression results in the observed defects in both processes. This may be attributable to the binding of the ParAB complex to an incorrect location in the cell, or it may indicate that the activity of the ParAB complex is modulated by other cell cycle events such as DNA replication or cell division. Increasing the amount of ParAB in the cell essentially results in uncoupling the processes of cell division and chromosome partitioning, perhaps indicating that these proteins have a critical role in coordinating cell cycle events.

The cell cycle–dependent spatial distribution of ParA and ParB in C. crescentus is strikingly reminiscent of proteins involved in eukaryotic mitosis. For example, ParB binds to DNA sequences adjacent to the origin of replication, suggesting that these sequences may function in a centromere-like fashion. Cell cycle immunolocalization experiments show that before the onset of DNA replication, ParB is distributed throughout the cell. Following the progression of DNA replication, ParB, possibly complexed with ParA, localizes to one pole of the predivisional cell (Figure 7). As replication and the cell cycle continue, ParB localizes to the opposite pole. The bipolar localization of ParB (Spo0J) has also been observed in both sporulating and vegetative cultures of B. subtilis (D. C.-H. Lin et al., submitted; P. Glaser et al., submitted). In C. crescentus, bipolar localization is shortly followed by the completion of cell division, whereupon the ParAB complex dissociates from the poles. We hypothesize that these events function to deliver the nascent chromosomes sequentially to opposite poles of the cell.

From these results, we make several general predictions regarding the role of ParA and ParB in DNA partitioning in bacterial cells. First, ParA and ParB are likely to be directly involved in directing the movement of chromosomal DNA toward the cell poles. This idea is supported by the fact that both *parA* and *parB* are essential genes in C. crescentus. In addition, the increased expression and resulting mislocalization of each of these gene products disrupt the movement of the chromosomes. Since neither ParA nor ParB has homology to motor-like proteins, we speculate that their role in chromosome movement is indirect, perhaps functioning in the attachment of the chromosomes to the cell envelope or to a motor protein such as MukB. Second, it is possible that ParA and ParB have a role in coordinating cell division with chromosome movement since the increased expression of these proteins also results in a cell division defect. ParA and ParB may function in the regulation of cell division by providing the cell with a mechanism to sense the arrival of the chromosomes at the cell poles. In this case, a process akin to a cell cycle checkpoint would prevent cell division until the chromosomes are correctly positioned at the poles. This checkpoint hypothesis is strengthened by the homology of ParA to the cell division regulator, MinD (DeBoer et al., 1991). The predicted amino acid sequence of C. crescentus *parA* shares 22% identity with that of *minD* from E. coli. The Min system prevents septum formation near the cell poles but permits septum formation at the midcell site. Therefore, the Min system can discriminate the poles of the cell from the midcell. ParA may function analogously by "sensing" the departure of the chromosomes from the midcell and their arrival at the poles. Both septum formation and partitioning are operationally analogous: spatial information within the cell is used to regulate a cell cycle–related event.

Third, ParA and ParB are likely to contribute to both the orientation and directionality of chromosome movement. Since ParB binds to DNA near the origin of replication, this critical region of the genome may be transiently tethered to the poles of the cell. This view is supported by genetic experiments in B. subtilis which demonstrated that the smaller forespore compartment initially receives the same segment of newly replicated DNA which contains sequences adjacent to the origin of replication (Wu and Errington, 1994; Wu et al., 1995; Sharpe and Errington, 1995, 1996). Furthermore, recent experiments have shown that the origin of replication in B. subtilis is localized at the poles of the cell (Webb et al., 1997). Mutations in *spo0J* result in random portions of the genome entering the forespore compartment, suggesting that *spo0J* plays a role in orienting the position of nascent chromosomes during the partitioning process (Sharpe and Errington, 1996).

Chromosome movement in bacteria is thought to be

accomplished either through nonspecific binding of the nascent chromosomes to the growing cell envelope (Woldringh and Nanninga, 1985; Begg and Donachie, 1991) or to a locomotor protein such as MukB (Hiraga et al., 1989; Niki et al., 1991, 1992). These models do not adequately take into account the issue of directionality during chromosome movement. How are the newly replicated chromosomes oriented so that they move to opposite poles of the cell? We propose that ParA and ParB may play a critical role in this process by initially selecting a single pole to which one chromosome is tethered, thereby providing directionality for the movement of the other newly replicated chromosome to the opposite pole of the cell. Based on these observations, we speculate that ParA and ParB function as one component in the bacterial equivalent of a mitotic apparatus.

Experimental Procedures

Isolation of the C. crescentus Homologs of *parA* and *parB*

C. crescentus *parA* was cloned using polymerase chain reaction (PCR). The primers corresponded to DNA encoding amino acid residues 10 to 17 (KGGVGKTT) and 123 to 129 (IDCPPSL). These regions are conserved in both B. subtilis (Mysliwiec et al., 1991) and Ps. putida homologs (Ogasawara and Yoshokawa, 1992). The PCR conditions were 35 cycles of 95°C for 1 min, 50°C for 2 min and 72°C for 3 min. The 357 bp PCR product was subcloned into M13 and sequenced. This product was used as a probe to screen a partial HindIII library of C. crescentus DNA in Bluescript KS (Stratagene) as well as a cosmid bank. *parA* and *parB* DNA was sequenced on both strands using dideoxy termination (Sanger et al., 1977). In order to map their genomic location *parAB* coding DNA was hybridized to a Southern blot of a pulse-field gel (CHEF gel apparatus, Bio-Rad). *parAB* hybridized to a 330 kb SpeI fragment, an 83 kb AseI fragment, and a 305 kb DraI fragment, placing it adjacent to the origin of replication (Ely and Gerardot, 1988; Dingwall and Shapiro, 1989; Marczynski and Shapiro, 1992). The *parA* and *parB* DNA sequence is deposited in GenBank (accession number U87804). Sequence comparisons were made using the BLAST algorithm (Altschul et al., 1990).

Purification of ParA and ParB

In order to overexpress ParB for purification, a BamHI restriction site was introduced adjacent to the ATG start codon by PCR. The resulting PCR fragment was cloned into the E. coli expression vector ptrcHisA (Invitrogen) creating an in-frame protein fusion. Expression of his-ParB was induced by the addition of 1 mM IPTG to a 0.5 l mid–log phase culture. The induced culture was harvested after 180 min at 37°C. Cells were resuspended in 20 mM Tris (pH 7.5), 0.5 M NaCl, 5 mM imidazole, 100 μM PMSF, and the cells were lysed with a French pressure cell. The resulting extract was centrifuged at 18,000 × g for 30 min at 4°C. The supernatant was loaded onto a 3 ml nickel-sepharose column and washed with 10 column volumes of 20 mM Tris (pH 7.5), 0.5 M NaCl, and 50 mM imidazole. His-ParB was eluted in a single step with 20 mM Tris (pH 7.5), 0.5 M NaCl, and 500 mM imidazole and dialyzed against 20 mM HEPES (pH 7.6), 0.1 mM EDTA, 12.5 mM $MgCl_2$, and 10% glycerol. His-tagged ParA was purified in essentially the same manner as his-ParB.

Gel mobility shift assay using purified ParB was performed as described previously (Wingrove et al., 1993) except the reaction buffer (30 μl total volume) also contained 0.3 μg/μl sheared salmon sperm DNA, 1.8 μg/μl single-stranded oligonucleotide DNA of the sequence 5′ GTCAAGCTACGGTTCTTG and 3 mg/ml bovine serum albumin. A 420 bp XhoI end-labeled fragment of *parS* DNA was added to a final concentration of 2.5 nM. To test for binding to unrelated A+T-rich DNA sequences, an end-labeled 280 bp HindIII-BamHI *fliF* operon fragment was used (Wingrove and Gober, 1994).

Cell Cycle Experiments

In order to assay the temporal expression of *parAB* operon, a *lacZ* fusion to a SalI fragment containing the *parA* upstream region and extending 320 bp into the parA coding region was constructed and integrated into the genome by homologous recombination. Cells were synchronized as described previously (Evinger and Agabian, 1977). Isolated swarmer cells were resuspended in M2 medium and permitted to progress through the cell cycle. At various time points, an aliquot was removed and the proteins were labeled with ^{35}S-*trans* label (ICN); β-galactosidase was immunoprecipitated as described previously (Gomes and Shapiro, 1984). For cell cycle immuonblots, isolated swarmer cells were resuspended in PYE medium (Poindexter, 1964) and permitted to progress through the cell cycle. At various time points, 1.0 ml samples were removed and the cells were centrifuged and suspended in 0.1 ml SDS-PAGE sample buffer; 50 ml was subjected to electrophoresis. Following electrophoresis, the separated proteins were subjected to immunoblot as described (Towbin et al., 1979).

Immunofluorescence Microscopy

Immunofluorescence microscopy was performed essentially as described (Maddock and Shapiro, 1993). Synchronized cultures grown in PYE were fixed with 0.1% glutaraldehyde, 3% formaldehyde in 20 mM sodium phosphate (pH 7.0) for 30 min at 0°C; they were washed three times with buffer containing 140 mM NaCl, 3 mM KCl, 8 mM Na_2HPO_4, 1.5 mM KH_2PO_4 and 0.05% Tween-20 (PBST) and resuspended in buffer containing 50 mM glucose, 10 mM EDTA, 20 mM Tris-HCl (pH 7.5) and 3 mg/ml lysozyme. Twenty milliliters of this suspension was placed onto polylysine-treated slides for 1 hr; slides were rinsed with distilled water and immediately placed into cold methanol for 5 min and cold acetone for 30 s, allowed to dry, rinsed with distilled water, and allowed to dry again. Samples were blocked for 20 min in PBST containing 2% bovine serum albumin and then incubated with antibody in PBST. Secondary antibody was goat anti-rabbit IgG conjugated to either fluorescein or biotin. In the case of biotin-conjugated secondary antibody, antigen-antibody complexes were then incubated with streptavidin-conjugated Texas red. In some cases the cells were also stained with propidium iodide (1 μg/ml), which stains cell membranes in addition to DNA in C. crescentus. Digital images were acquired with an Optronics cooled CCD camera and captured with Adobe Photoshop.

To epitope tag ParA, a BamHI restriction site was introduced adjacent to amino acid 291 by PCR. The PCR product was cloned into pJM21 (Alley et al., 1993; Wingrove and Gober, 1996) creating a M2 epitope protein fusion at the carboxyl terminus of ParA. The *parA*-M2 fusion was introduced into C. crescentus by conjugation. ParA-M2 immunofluorescence experiments were performed with monoclonal anti-FLAG (Kodak) antibody as described above except in this case goat anti-mouse antibody conjugated to fluorescein was used as a secondary antibody. As a control, immunofluorescence was also performed on cells expressing a *gyrB-lacZ* transcriptional fusion.

Cells were stained with 4,6-diamidino-2-phenylindole (DAPI) in order to visualize chromosomal DNA. Cell suspensions were treated as described for immunofluorescence except the fixation time was extended to 45 min. Slides were covered with 4 μl of a solution containing 50% glycerol and 1 μg/ml DAPI. DNA was visualized with combined phase contrast and fluorescence microscopy in order to visualize individual chromosomes (Hiraga et al., 1989).

Acknowledgments

We thank M. E. Sharpe, J. Errington, A. Grossman, R. Losick, and A. Wright for sharing data prior to publication. We are also grateful to members of our laboratory for helpful comments on the manuscript. This work was supported by a grant from the National Science Foundation (MCB-9513222) and a Junior Faculty Research Award (JFRA-466) from the American Cancer Society to J. W. G. Initial portions of this work were supported by Public Health Service Grant GM48417 from the National Institutes of Health.

Received December 27, 1996; revised February 19, 1997.

References

Alley, M.R.K., Maddock, J., and Shapiro, L. (1993). Requirement of the carboxyl terminus of a bacterial chemoreceptor for its targeted proteolysis. Science *259*, 1754–1757.

Altschul, S.F., Gish, W., Moller, W., Myers, E.W., and Lipman, D.J. (1990). Basic local alignment search tool. J. Mol. Biol. *215*, 403–410.

Austin, S., and Abeles, A. (1983a). Partition of unit-copy miniplasmids to daughter cells. I. P1 and F miniplasmids contain discrete, interchangeable sequences sufficient to promoter equipartition. J. Mol. Biol. *169*, 353–372.

Austin, S., and Abeles, A. (1983b). Partition of unit-copy miniplasmids to daughter cells. II. The partition region of miniplasmid P1 encodes an essential protein and a centromere-like site at which it acts. J. Mol. Biol. *169*, 373–387.

Begg, K.J., and Donachie, W.D. (1991). Experiments on chromosome separation and positioning in *Escherichia coli.* New Biol. *3*, 475–486.

Dam, M., and Gerdes, K. (1994). Partitioning of plasmid R1. Ten direct repeats flanking the *par* promoter constitute a centromere-like site, *parC*, that expresses incompatibility. J. Mol. Biol. *236*, 1289–1298.

Davis, M.A., and Austin, S.J. (1988). Recognition of the P1 plasmid centromere analog involved binding of the ParB protein and is modified by a specific host factor. EMBO J. *7*, 1881–1888.

Davis, M.A., Martin, K.A., and Austin, S. (1992). Biochemical activities of the ParA partition protein of the P1 plasmid. Mol. Microbiol. *6*, 1141–1147.

DeBoer, P.A.J., Crossley, R.E., Hand, A.R., and Rothfield, L.I. (1991). The MinD protein is a membrane ATPase required for the correct placement of the *Escherichia coli* cell division site. EMBO J. *10*, 4371–4380.

Dingwall, A., and Shapiro, L. (1989). Rate, origin, and bidirectionality of *Caulobacter* chromosome replication as determined by pulsed-field gel electrophoresis. Proc. Natl. Acad. Sci. USA *86*, 119–123.

Ely, B., and Gerardot, C.J. (1988). Use of pulsed-field-gradient gel electrophoresis to construct a physical map of the *Caulobacter crescentus* genome. Gene *68*, 323–333.

Evinger, M., and Agabian, N. (1977). Envelope-associated nucleoid from *Caulobacter crescentus* stalked and swarmer cells. J. Bacteriol. *132*, 294–301.

Gerdes, K., and Molin, S. (1986). Partitioning of plasmid R1. Stuctural and functional analysis of the parA locus. J. Mol. Biol. *190*, 269–279.

Gober, J.W., and Marques, M.V. (1995). Regulation of cellular differentiation in *Caulobacter crescentus*. Microbiol. Rev. *59*, 31–47.

Gomes, S.L., and Shapiro, L. (1984). Differential expression and positioning of chemotaxis methylation proteins in *Caulobacter*. J. Mol. Biol. *178*, 551–568.

Higgins, D.G., and Sharp, P.M. (1989). CLUSTAL: a package for performing multiple sequence alignment on a microcomputer. Gene *73*, 237–244.

Hiraga, S. (1992). Chromosome and plasmid partitioning in E. coli. Annu. Rev. Biochem. *61*, 283–306.

Hiraga, S., Niki, H., Ogura, T., Ichinose, C., Mori, H., Ezaki B., and Jaffé, A. (1989). Chromosome partitioning in *Escherichia coli*: novel mutants producing anucleate cells. J. Bacteriol. *171*, 1496–1505.

Ireton, K., Gunther, N.W., and Grossman, A.D. (1994). *spo0J* is required for normal chromosome segregation as well as the initiation of sporulation in *Bacillus subtilis*. J. Bacteriol. *176*, 5320–5329.

Maddock, J.R., and Shapiro, L. (1993). Polar localization of the chemoreceptor complex in the *Escherichia coli* cell. Science *259*, 1717–1723.

Marczynski, G.T., and Shapiro, L. (1992). Cell-cycle control of a cloned chromosomal origin of replication from *Caulobacter crescentus*. J. Mol. Biol. *226*, 959–977.

Martin, K.A., Friedman, S.A., and Austin, S.J. (1987). Partition site of the P1 plasmid. Proc. Natl. Acad. Sci. USA *84*, 8544–8547.

Meisenzahl, A.C., Shapiro, L., and Jenal, U. (1997). Isolation and characterization of a xylose-dependent promoter from Caulobacter crescentus. J. Bacteriol., in press.

Mori, H., Mori, Y., Ichinose, C., Niki, H., Ogura, T., Kato, A., and Hiraga, S. (1989). Purification and characterization of SopA and SopB proteins essential for F plasmid partitioning. J. Biol. Chem. *264*, 15535–15541.

Mysliwiec, T.H., Errington, J., Vaidya, A.B., and Bramucci, M.G. (1991). The *Bacillus subtilis spo0J* gene: evidence for involvement in catabolite repression of sporulation. J. Bacteriol. *173*, 1911–1919.

Niki, H., Jaffé, A., Imamura, R., Ogura, T., and Hiraga, S. (1991). The new gene *mukB* codes for a 177 kd protein with coiled-coil domains involved in chromosome partitioning of E. coli. EMBO J. *10*, 183–193.

Niki, H., Imamura, R. , Kitaoka, M., Yamanaka, K., Ogura, T., and Hiraga, S. (1992). *E. coli mukB* protein involved in chromosome partition forms a homodimer with a rod-and-hinge structure having DNA binding and ATP/GTP binding activities. EMBO J. *13*, 5101–5109.

Ogasawara, N., and Yoshokawa, H. (1992). Genes and their organization in the replication origin region of the bacterial chromosome. Mol. Microbiol. *6*, 629–634.

Poindexter, J.S. (1964). Biological properties and classifications of the *Caulobacter* group. Bacteriol. Rev. *28*, 231–295.

Rothfield, L.I. (1994). Bacterial chromosome segregation. Cell *77*, 963–966.

Sanger, F., Nicklen, S., and Coulson, A.R. (1977). DNA sequencing with chain terminating inhibitors. Proc. Natl. Acad. Sci. USA *74*, 5463–5467.

Schmidhauser, T.J., Bechhofer, D.H., Figurski, D.H., and Helinski, D.R. (1989). Host-specific effects of the *korA-korB* operon and *oriT* region on the maintenance of miniplasmid derivatives of broad host-range plasmid RK2. Plasmid *21*, 99–112.

Sharpe, M.E., and Errington, J. (1995). Post-septational chromosome partitioning in bacteria. Proc. Natl. Acad. Sci. USA *92*, 8630–8634.

Sharpe, M.E., and Errington, J. (1996). The *Bacillus subtilis soj-spo0J* locus is required for a centromere-like function involved in prespore chromosome partitioning. Mol. Microbiol. *21*, 501–509.

Towbin, H., Staehlin, T., and Gordon, J. (1979). Electrophoretic transfer of proteins from polyacrylamide gels to nitrocellulose sheets: procedure and some applications. Proc. Natl. Acad. Sci. USA *76*, 4350–4354.

Wake, R.G., and Errington, J. (1995). Chromosome partitioning in bacteria. Annu. Rev. Genet. *29*, 41–67.

Watanabe, E., Wachi, M., Yamasaki, M., and Nagai, K. (1992). ATPase activity of SopA, a protein essential for active partitioning of F plasmid. Mol. Gen. Genet. *234*, 346–352.

Webb, C.D., Teleman, A., Gordon, S., Straight, A., Belmont, A., Lin, D.C.-H., Grossman, A.D., Wright, A., Losick, R. (1997). Bipolar localization of the replication origin regions of chromosomes in vegetative and sporulating cells of B. subtilis. Cell, this issue.

Wingrove, J.A., and Gober, J.W. (1994). A σ^{54} transcriptional activator also functions as a pole-specific repressor in *Caulobacter*. Genes Dev. *8*, 1839–1852.

Wingrove, J.A., and Gober, J.W. (1996). Identification of an asymmetrically localized sensor histidine kinase responsible for temporally and spatially regulated transcription. Science *274*, 597–601.

Wingrove, J.A., Mangan, E.K., and Gober, J.W. (1993). Spatial and temporal phosphorylation of a transcriptional activator regulates pole-specific gene expression in *Caulobacter*. Genes Dev. *7*, 1979–1992.

Woldringh, C.L., and Nanninga, N. (1985). Structure of the nucleoid and cytoplasm in the intact cell. In Molecular Cytology of *Escherichia coli*, N. Nanninga, ed. (Academic Press: New York), pp. 161–197.

Wu, L.J., and Errington, J. (1994). Bacillus subtilis SpoIIIE protein required for DNA segregation during asymmetric cell division. Science *264*, 572–575.

Wu, L.J., Lewis, P.J., Allmansberger, R., Hauser, P.M., and Errington, J. (1995). A conjugation-like mechanism for prespore chromosome partitioning during sporulation in *Bacillus subtilis*. Genes Dev. *9*, 1316–1326.